Journal of Chemical Health Risks

www.jchr.org

JCHR (2024) 14(1), 1980-1986 | ISSN:2251-6727

Preparation, Characterization and Evaluation of Copper Oxide Nanoparticles

Rahul Ratnakar Mahamuni, Department of Conservation of Biodiversity, Gopinathrao Munde National Institute of Rural Development and Research- A Constitute Institute of Dr. Babasaheb Ambedkar Marathwada University, Chhatrapati Sambhajinagar (formerly Aurangabad), Maharashtra.

S.Tamizharasi, PG Department of Chemistry, Marudhar Kesari Jain College for Women, Vaniyambadi Tirupattur, Tamilnadu.

B.Latha, Department of Physics, Rajalakshmi Engineering College (Autonomous), Thandalam, Tamilnadu.

M. Charumathy, PG & Research Department of Biochemistry, Marudhar Kesari Jain College for Women, Vaniyambadi, Tirupattur, Tamilnadu.

R. Venkateswari, Department of Medical Biochemistry, University of Madras, Taramani Campus, Chennai, Tamilnadu.

Harishchander Anandaram, Amrita School of Artificial Intelligence, Coimbatore, Amrita Vishwa Vidyapeetham, Tamilnadu.

(Received: 05 November 2023 Revised: 12 December Accepted: 07 January)

KEYWORDS

Stroke copper nanoparticles, *Mangifera indica*, agar well diffusion method.

Abstract

Because of their potential applications in optoelectronics, nanoelectronics, sensors, catalysis, and information storage, metal oxide nanoparticles, or NPs, are the subject of much research. Using *Mangifera indica* leaf extract, the study sought to investigate the synthesis of CuO nanoparticles (NPs) and evaluate their properties. It was established whether Mangifera indica leaf extract was suitable for utilising a biological process in ambient conditions to produce copper oxide nanoparticles. The spherical-shaped CuO nanoparticles are polydisperse, with a range of particle sizes from 18 to 106 nm. 52.54 nm was the average size. Colour changes indicate the generation of CuO nanoparticles (NPs) through plasmon resonance with the bioactive compounds in the Mangifera indica leaf extract. FT-IR, UV-vis spectroscopy, XRD, EDX, and SEM methods were also used to confirm the presence of CuO nanoparticles. As a capping agent and aiding in the bio reduction process, the functional groups have been shown to have a probable affinity for copper oxide. This affinity is seen with alkynes, aromatics, phenol, and alcohol. The agar well diffusion method was used to evaluate the antibacterial effectiveness of the generated copper nanoparticles and to identify the lowest inhibitory concentration. The zone of inhibition could be anywhere between 10 and 30 mm in length. However, depending on the particular organism under investigation, the bactericidal effectiveness of copper nanoparticles varies.

Introduction

One important area of study is nanotechnology, which is the creation and manipulation of materials whose structures lie between those of individual atoms and bulk materials, frequently having at least one dimension in the nanoscale range. Because of their potential uses in nanotechnology, optoelectronics, sensors, electronics, catalysis, and information storage, metallic oxide nanoparticles, or NPs, are being researched in great detail. When compared to other metal nanoparticles, copper oxide nanoparticles are highly valuable because of their remarkable chemical and physical properties and low cost of production. Copper oxide nanoparticles are widely used as catalysts, antimicrobial agents, heat conductors, extremely durable materials, and sensors. The high surface-to-volume ratio of copper oxide nanoparticles makes them highly reactive, which increases their antibacterial activity by allowing them to easily interact with other particles [1-3]. Historically, physical and chemical methods have been used in the production of nanoparticles. On the other hand, biological approaches have become increasingly popular recently. Chemical processes have a number of drawbacks, including the production of toxic byproducts, excessive energy consumption, and the use of solvents that are harmful to the environment and public health. Hence, when it comes to manufacturing nanoparticles, the green method is more cost-effective

Journal of Chemical Health Risks

www.jchr.org

JCHR (2024) 14(1), 1980-1986 | ISSN:2251-6727

and environmentally friendly than physical and chemical methods [4]. Plant extracts and microorganisms are used in the environmentally friendly process of producing nanoparticles [5]. The use of plants and materials derived from plants in the synthesis of nanoparticles has gained more attention recently. CuO nanoparticle production from different plants and their derivatives has been the subject of several investigations [6–8]. Therefore, we evaluated the synthesis and analysis of CuO nanoparticles using Mangifera indica leaf extract in this study.

Experimental Methods

Preparation of Leaves Extract

Harvested were the undamaged foliage of robust *Mangifera indica* plants. The dust particles adhering to the leaves were eliminated by rinsing them with water and thereafter allowing them to air dry in a shaded area for a duration of two weeks. A 10 g quantity of dried fine leaf powder from *Mangifera indica* was combined with 400 mL of sterile distilled water in a 500 mL beaker to prepare the aqueous extract. The color of the aqueous solution transformed from clear to a brown-yellow hue after being cooked for 10 minutes. Next, the mixture was passed through a Whatman No. 1 filter paper to separate the biomaterials. The resulting filtrate was then subjected to centrifugation at a speed of 1200 revolutions per minute for a duration of 5 minutes to remove any remaining biomaterials. The extract was preserved for subsequent experimentation.

Copper Oxide Nanoparticle (CuO NPs) Synthesis

The copper acetate monohydrate, weighing 2.8 grams, was dissolved in 500 milliliters of deionized water. The mixture was agitated using a magnetic stirrer for a duration of 5 minutes at room temperature. Subsequently, the *Mangifera indica* leaves aqueous extract was slowly added drop by drop while stirring, immediately upon contact with copper ions, resulting in a color transformation from blue to green. After a duration of 10 minutes, the emergence of water-soluble copper oxide nanoparticles that are uniformly disseminated as individual particles was detected [9].

Characterization of Nanoparticles

UV and FTIR Spectroscopic Analysis

The Perkin Elmer Spectrophotometer was used to analyze the reduction of pure Cu+ ions in the wavelength range of 260-900 nm for UV and FTIR spectrophotometer analysis. The resulting data revealed the presence of distinctive peaks. The FTIR analysis was conducted utilizing a Spectrophotometer instrument to identify the characteristic peaks within the range of 400-4000 cm-1 and determine their corresponding functional groups. The maximum values of the ultraviolet (UV) and Fourier-transform infrared (FTIR) were recorded.

Electron Microscopy and EDX Analysis of Copper Oxide Nanoparticles

The ZEEISS-SEM equipment was utilized to analyze the average particle size and shape of CuO nanoparticles. The samples were rendered conductive by applying a thin layer of platinum coating. The ZEEISS-SEM machine was operated at a vacuum condition of approximately 10-5 torr. The microscope maintained an accelerating voltage within the range of 10 kilovolts. The sample underwent compositional analysis using energy dispersive X-ray spectroscopy (EDS) in conjunction with the scanning electron microscope (SEM). The Cu sample was subjected to EDX examination using the SEM equipment.

X-Ray Diffraction Method

The X-ray diffraction technique was used to analyze the phase evolution of both the calcined powder and the sintered samples. The analysis was conducted using a Philips Analytical X-ray diffractometer system (Model: PW3040/60 XPERT-PRO) from the Netherlands, with monochromatic CuKα radiation of wavelength 1.5418 Å. The voltage and current of the generator were adjusted to 40 kilovolts and 30 milliamperes, respectively. The scanning range $2\theta/\theta$ was chosen. A scanning speed of 10 min−1 was used for accurate determination.

Antimicrobial activity

The antibacterial efficacy of the produced CuONPs was assessed against Escherichia coli, Staphylococcus aureus, serratia species, and Vibrio harveyi using the disc diffusion method. Subsequently, the antifungal efficacy was assessed against Aspergillus niger and Aspergillus fumigatus. The nutrient agar plates were inoculated with bacterial and fungal cultures that had been incubated overnight. On the inoculated plates, 50 µL of biosynthesized CuONPs with varying concentrations (ranging from 250 to 1000 µg/mL) were applied. Following a period of incubation at a temperature of 37°C for a duration of 24 hours, the diameters of the zones were measured in millimeters.

Results and Discussion

Copper Oxide Nanoparticle Synthesis

The production of copper oxide nanoparticles

Journal of Chemical Health Risks

www.jchr.org

JCHR (2024) 14(1), 1980-1986 | ISSN:2251-6727

using the extract of *Mangifera indica* leaves was conducted in this study. Upon eye examination, the combination of copper acetate and magnetically swirled leaf extract exhibited a green mixture after a duration of 10 minutes. The transformation of copper ions from blue to green hue serves as a distinct sign of the formation of water-soluble, uniformly dispersed copper oxide nanoparticles.

UV-VIS Spectral Analysis

It is widely acknowledged that UV-Vis spectroscopy is used to analyze size and shape-controlled nanoparticles in aqueous solutions. The UV-Vis spectra were reported in Figure 1. The UV–Vis spectra of the reaction mixture containing *Mangifera indica* leaf extract and copper acetate solution showed a peak at 284 nm, suggesting the completion of the reduction of copper acetate monohydrate and the generation of CuO NPs. This process took around 10 minutes at room temperature. The peak was elevated as a result of interband transitions of core electrons in the CuO nanoparticles inside the reaction mixture. The broadening of the peak suggests the presence of polydisperse particles. The absorption wavelength values are consistent with previously published values [6-9].

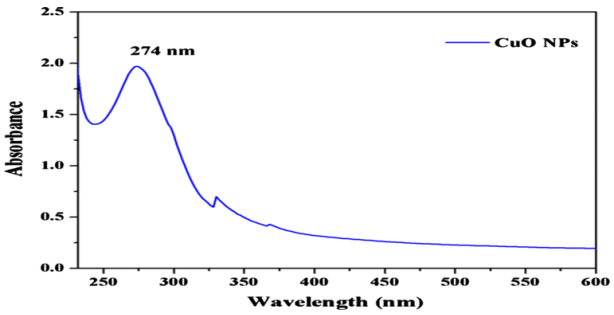

Fig. 1 UV-Vis Spectral analysis of CuONPs

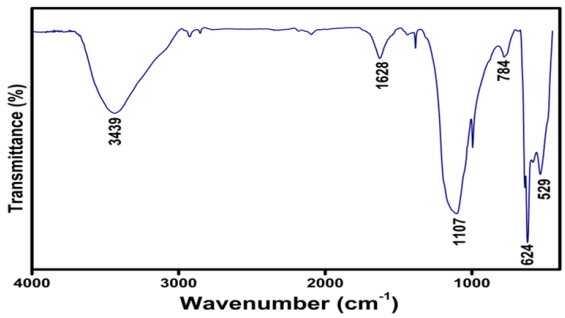

Fig. 2 FTIR spectrum of copper oxide nanoparticles synthesized by reduction of Cu^{+} ions by *Mangifera indica* leaves extract

Fourier Transform Infra-Red Spectral Analysis of CuO NPs

The FTIR spectrum of copper oxide nanoparticles was analyzed to determine the bioactive components that are responsible for the capping and effective stability of the copper oxide nanoparticles generated from the extract of leaves. The peaks detected in Figure 2, at 3439.91 cm−1 (representing Alcohol and Phenol), 1638.27 cm−1 (indicating aromatic rings), and 668.76 cm-1 (corresponding to alkynes), provide evidence for the existence of flavonoids and phenols that are attached to the surface of copper oxide nanoparticles produced through the reduction process using *Mangifera indica* leaves. The FTIR study confirmed the presence of alcohol, phenol, aromatics, and alkynes compounds. This analysis demonstrated that the sample contained secondary metabolites, which functioned as predicted capping and stabilizing agents.

Scanning and Transmission Electron Microscope (SEM) Analysis of CuO NPs

The size and structure of the CuO NPs were analyzed using SEM and TEM techniques, revealing the synthesis of polydisperse spherical copper-NPs of varying sizes and increased density. The SEM investigation revealed that the nanoparticles had a size range of 86.24 - 94.44 nm and exhibited both spherical and crystalline characteristics. The majority of the nanoparticles aggregated while just a small portion of them exhibited dispersion, as revealed using SEM.

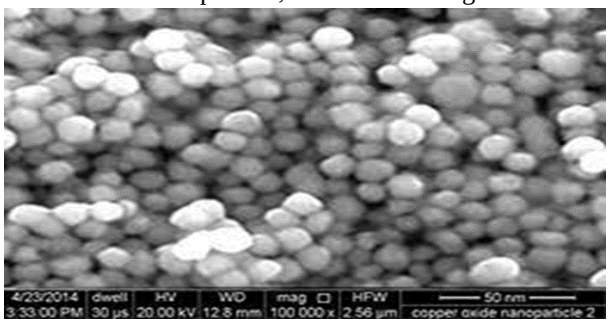

Fig. 3 High resolution scanning electron microscopic (SEM) image of copper oxide nanoparticles (CuONPs). polydispersed (Cluster) CuO NPs ranged between 86.24 - 94.44 nm

Energy-Dispersive X-Ray Spectroscopy (EDX) Analysis of CuO NPs

The data provided by EDX analysis comprises spectra featuring peaks corresponding to each element present in the sample. The Energy Dispersive Spectroscopy (EDS) analysis of CuO nanoparticles

Journal of Chemical Health Risks

www.jchr.org

JCHR (2024) 14(1), 1980-1986 | ISSN:2251-6727

indicated the predominance of copper (Cu) as the main constituent element, accounting for 98.74% of the composition. Carbon (C) constituted only 1.26% of the composition, as shown in Table 1 and Figure 4. The EDX analysis confirmed the presence of the obligatory copper (Cu) phase in the CuO NPs.

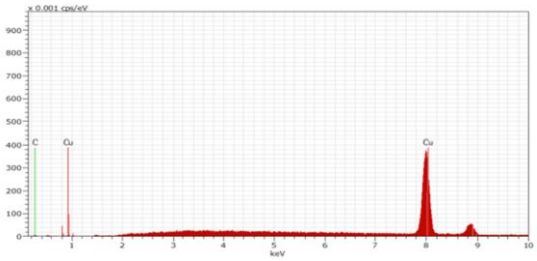

Fig. 4 EDS-spectroscopy view of the *Mangifera indica* showing synthesis of copper oxide nanoparticles and elemental copper signal in higher percentage

Table 1 Percentage of elements present in the CuO NPs

Elements	AN	Series	Weight %	Atomic %
Cu	29	K -series	98.74	93.70
C	06	K-series	1.26	6.30
Total			100	100

The XRD Pattern of CuO NPs Synthesized from Leaves

X-ray diffraction (XRD) is commonly employed to determine the crystal structure and chemical makeup of a substance. Hence, the detection of copper oxide nanoparticles can be accomplished by employing X-ray diffraction (XRD) to analyze the diffraction patterns of the CuO NPs. The figure displays the X-ray diffraction pattern of CuO nanoparticles. The crystalline nature of Cu nanoparticles was confirmed using X-ray diffraction (XRD) analysis, which revealed the XRD pattern of the dried nanoparticles derived from colloid samples. The presence of Bragg reflections at specific 2θ values, namely 31.41, 38.20, 46.07, 64.42, 67.49, and 77.20O, confirms the existence of the (110), (111), (200), (220), (300), and (311) reflections of metallic copper. These reflections clearly indicate that copper possesses a cubic crystalline face-centered cubic structure. This conclusion was drawn by comparing the observed reflections with the reference data from the JCPDS card 05-0661, which is a standard powder diffraction card. The constant value is 28.81, which is obtained by subtracting 47.1564 from 75.974. The XRD pattern clearly demonstrates that the copper oxide nanoparticles synthesized in this study had a crystalline structure. The broadening of the peaks is mostly caused by the diminutive particle size. The process of indexing has been completed and the data may now be found in Table 2.

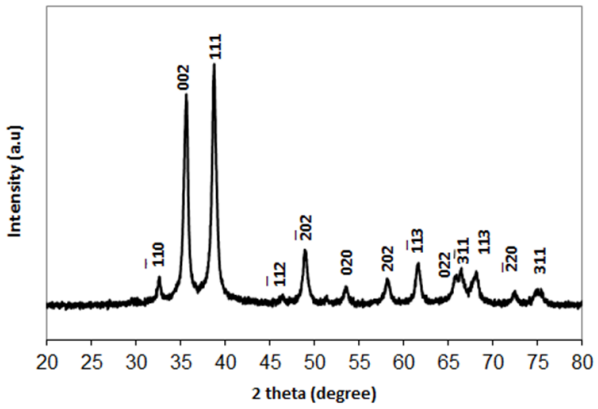

Fig. 5 XRD patterns of copper nanoparticles synthesized using leaves

Table 2 Simple peak indexing

Peak (2θ)	1000 × Sin2θ	1000 × Sin2θ/28.80	Reflection	Remarks
18.87	47.15640956	1	100	$1^2 + 0^2 + 0^2 = 1$
24.02	75.96025967	2	110	$1^2 + 1^2 + 0^2 = 2$
29.20	111.4824095	3	111	$1^2 + 1^2 + 1^2 = 3$
31.71	130.9900266	4	200	$2^2 + 2^2 + 0^2 = 4$
37.83	184.3575903	6	211	$2^2 + 1^2 + 1^2 = 6$
43.4	239.8452168	8	220	$2^2 + 2^2 + 0^2 = 8$
47.52	284.8088832	10	310	$3^2 + 1^2 + 0^2 = 10$

Journal of Chemical Health Risks

www.jchr.org

JCHR (2024) 14(1), 1980-1986 | ISSN:2251-6727

50.46	318.7607155	11	311	$3^2 + 1^2 + 1^2 = 11$
56.4	13.9910883 2	14	320	$3^2 + 2^2 + 1^2 = 14$

Table 3 The copper oxide nanoparticle grain size

Intense peak 2θ (deg)	Miller indices (hkl)	θ of the intense peak (deg)	FWHM of intense peak (β) radians	Size of the particle (D) nm
18.87	100	9.435	0.164672	49.5371
24.02	110	12.01	0.209615	45.37157
29.20	111	14.6	0.254819	78.80114
31.71	200	15.855	0.276723	29.20921
37.83	211	18.915	0.33013	24.38523
43.4	220	21.7	0.378737	22.27469
47.52	310	23.76	0.414691	98.00582
50.46	311	25.23	0.440348	18.3367
56.40	320	28.20	0.492184	106.9842
Average nanoparticle size				52.5450

Particle Size Calculation

This work utilized the Debye-Scherrer formula to estimate the average particle size based on the peak observed at several degrees [10-13]. The formula, $D = 0.9 \lambda/\beta \cos \theta$, involves the variables 'λ' which represents the wavelength of X-Ray (0.1541 nm), 'β' which represents the full width at half maximum (FWHM), 'θ' which represents the diffraction angle, and 'D' which represents the diameter size of the particles. The Debye-Scherrer equation yielded an average crystalline size of 52.54 nm, which is presented in Table 3.

Antimicrobial activity

The synthesized CuONPs were assessed for their antibacterial efficacy against E. coli, S. aureus, Serratia Sp, and V. harveyi bacteria. The CuONPs exhibited antimicrobial efficacy against all the species tested, as shown in Table 1. The study revealed a positive correlation between the concentration of CuONPs and the size of the zone of inhibition, as depicted in Figure 5. The precise mechanism behind the biocidal activity of CuONPs remains incompletely understood. Ruparelia et al. (2008) and Wu et al. (2009) proposed that copper ions from CuONPs could potentially interact with phosphorus and sulfur-containing biomolecules, such as DNA and proteins, leading to structural distortions and subsequent disruption of metabolic processes. The efficacy of CuONPs against both Gram-negative and Gram-positive bacteria suggests their potential as a broad-spectrum nanoparticle. The creation of cell filaments induced by CuONPs leads to the breakdown of bacterial cell membranes, resulting in the suppression of bacterial colony growth (Montes-Burgos et al., 2010; Saranya et al., 2020).

The antifungal efficacy of CuO nanoparticles was assessed by cultivating Aspergillus niger and Aspergillus fumigatus on agar CD media supplemented with varying concentrations of CuO nanoparticles (Figure 5). The study revealed that the growth of A. niger and Aspergillus fumigatus was hindered in a manner that depended on the concentration of the substance. This information can be seen in Table 2. The latest breakthroughs in nanotechnology, specifically the capability to synthesize metal oxide nanoparticles with precise dimensions and configurations, have the potential to pave the way for novel antifungal drugs. The utilization of nanoparticle (NP) technology indicates a novel and auspicious strategy for the treatment of fungal infections [14-19].

Table 1. Antibacterial activity of Phyto-synthesized CuONPs

Zone of Inhibition (mm)				
Concentration (µg/mL)				
Bacterial Strain	**Control**	**250**	**500**	**1000**
E. coli	13	14	15	18
S. aureus	30	15	23	30
Serratia sp	33	10	12	17
V. harveyi	24	13	14	15

Table 2. Antifungal activity of Phyto-synthesized CuONPs.

Zone of Inhibition (mm)				
Concentration (µg/mL)				
Fungi	**Control**	**250**	**500**	**1000**
A. niger	16	9	11	13
A. fumigatus	35	16	16	18

Journal of Chemical Health Risks

www.jchr.org

JCHR (2024) 14(1), 1980-1986 | ISSN:2251-6727

Conclusion

This study found that the aqueous extract of Mangifera indica leaf was used to create CuO nanoparticles using a straightforward and environmentally favorable green approach from copper acetate monohydrate. The CuO nanoparticles showed both polydispersity and a spherical form, with particle sizes ranging from 18 to 106 nm. 52.54 nm was found to be the average particle size. The antibacterial and antifungal activities of the copper oxide nanoparticles were remarkable.

References

1. T.I. Brunner, P. Wick, P. Manser, P. Spohn, R.N. Grass, et al., In vitro cytotoxicity of oxide nanoparticles: comparison to asbestos, silica, and effect of particle solubility, Env. Sci. Technol. 40 (2006) 4374-4381.
2. F. Marabelli, G.B. Parravicini, F. Salghetti-Drioli, Optical gap of CuO, Phys. Rev. B 52(3) (1995) 1433-1436.
3. R. Narayanan, El-Sayed, Effect of catalysis on the stability of metallic nanoparticles: Suzuki reaction catalyzed by PVP-palladium nanoparticles, J. Am. Chem. Soc. 125(27) (2003) 8340-8347.
4. Ahamed, M., Hisham, AA., Majeed Khan, MA., Karuppiah, P., Naif, A., Dhabi, A. (2014) Synthesis, characterization, and antimicrobial activity of copper oxide nanoparticles Journal of nanomaterials. 17: 1-4.
5. Baek, YW and An, YJ. (2011). Microbial toxicity of metal oxide nanoparticles (CuO, NiO, ZnO, and Sb2O3) to Escherichia coli, Bacillus subtilis, and Streptococcus aureus. Science of the Total Environment 409: 1603– 1608.
6. Gebremedhn, K,, Kahsay, MH., Aklilu, M. (2019). Green synthesis of CuO nanoparticles using leaf extract of catha edulis and its antibacterial activity Journal of Pharmacy Pharmacology. 7: 327–42
7. Gunalan, S., Sivaraj, R., and Venckatesh, R. (2012). Aloe barbadensis Miller mediated green synthesis of mono-disperse copper oxide nanoparticles: optical properties. Spectrochimica acta. Part A, Molecular and Biomolecular Spectroscopy 97: 1140-1144.
8. Hassanien, R., Dalal, Z., Husein, Mostafa, F., Hakkani, A (2018). Biosynthesis of coppernanoparticles using aqueous Tilia extract: antimicrobialand anticancer activities. Heliyon. 4: 1-21.
9. Heinlaan, M., Ivask, A., Blinova, I., Dubourguier, H., Kahru, A. (2012). Toxicity of nanosized and bulk ZnO, CuO and TiO2 to bacteria Vibro fischeri and crustaceans Daphyna magna and Thamnocephalus platyurus. Chemosphere 71: 1308–1316.
10. K. Nabhikha, A. Kathiersan, M. Raj, N. Alikunhi, Synthesis of antimicrobial copper nanoparticles by callus and leaf extract from salt marsh plants, *Sesuvium portulacastrum* L. Colloids Surf. Biointerf. 79 (2009) 488-493.
11. S. Prabhu, E.K. Poulose, Silver nanoparticles: mechanism of antimicrobial action, synthesis, medical applications, and toxicity effects, Int. Nano Lett. 2(1) (2012) 1-10.
12. R.K. Swarnkar, S.C. Singh, R. Gopal, Synthesis of copper/copper-oxide nanoparticles: optical and structural characterizations, AIP Conf. Proc. 1147 (2009) 205-209.
13. R. Abdul, Amri Ismail, Desi Jumbianti, Stella Magdalena, Hanggara Sudrajat, Synthesis of copper oxide nano particles by using *Phormidium cyanobacterium*, Indo. J. Chem. 9(3) (2009) 355-360.
14. S. Ansilin, J. Kavya Nair, C. Aswathy, V. Rama, J. Peter, J. Jeyachynthaya, Green synthesis and characterization of copper oxide nanoparticles using *Azadirachta indica* (Neem) leaf aqueous extract, J. Nanosci. Tech. 2(5) (2016) 221-223.
15. A.Y. Ghidan, M. Tawfiq Al-Antary, A.M. Awwad, Green synthesis of copper oxide nanoparticles using *Punica granatum* peels extract: Effect on green peach Aphid, Environ. Nanotechnol. Monitor. Manag. 6 (2016) 95-98.
16. R.W. Sun, C. Rong, N.P.Y. Chung, C.M. Ho, C.L.S. Lin, C.M. Che, Silver nanoparticles fabricated in Hepes buffer exhibit cytoprotective activities toward HIV-1 infected cells, Chem. Commun. 28 (2005) 5059-5061.
17. S.S. Nath, D. Chakdar, G. Gope, Synthesis of CdS and ZnS quantum dots and their applications in electronics, Nanotr. A J. Nanotech. Its Appl. 2 (2007) 230-236.
18. S.S. Nath, D. Chakdar, G. Gope, D.K. Avasthi, Effect of 100 MeV nickel ions on silica coated ZnS quantum dot, J. Nanoelect. Optoelect. 3 (2008) 1-4.

Journal of Chemical Health Risks

www.jchr.org

JCHR (2024) 14(1), 1980-1986 | ISSN:2251-6727

19. S. Bykkam, M. Ahmadipour, N. Sowmya, V.R. Kalagadda, S.C. Chidurala, Extensive studies on X-ray diffraction of green synthesized silver nanoparticles, Adv. Nanopart. 4 (2015) 1-10.